



Tenth U.S. National Conference on Earthquake Engineering
Frontiers of Earthquake Engineering
July 21-25, 2014
Anchorage, Alaska

DETECTION OF BUILDING SIDE-WALL DAMAGE CAUSED BY THE 2011 TOHOKU, JAPAN EARTHQUAKE TSUNAMIS USING HIGH-RESOLUTION SAR IMAGERY

W. Liu¹, M. Matsuoka², F. Yamazaki³, T. Nonaka⁴, and T. Sasagawa⁴

ABSTRACT

Building damage such as to side-walls or mid-story collapse is often overlooked in vertical optical images. Hence, in order to observe such building damage modes, high-resolution SAR images are introduced considering the side-looking nature of SAR. In the 2011 Tohoku, Japan, earthquake, a large number of buildings were collapsed or severely damaged due to repeated tsunamis. One of the important tsunami effects on buildings is that the damage is concentrated to their side-walls and lower stories. Thus, this paper proposes the method to detect this kind of damage from the change in layover areas in SAR intensity images. The pre- and post-event TerraSAR-X images covering the Sendai-Shiogama Port were employed to detect building damage due to the tsunamis caused by the earthquake. Firstly, a shape data of the layover areas for individual buildings were made according to the 2D Zenrin GIS data because the lengths of layover are proportional to the building height. The characteristics of the difference of backscattering coefficients between the pre- and post-event images were investigated for several sample buildings. Then the average value and the gradient in the cumulative distribution of the difference were used to classify the possibility of side-wall damage and the damage level of buildings. These examples demonstrated the usefulness of high-resolution SAR images to detect severe damage to building side-walls from the changes of the backscattering coefficient in layover areas. Finally, the method was applied to the whole target area, and the accuracy was verified by comparing with a building damage map made by field surveys.

¹Postdoctoral Fellow, Dept. of Built Environment, Tokyo Institute of Technology, Japan 226-8502

²Associate Professor, Dept. of Built Environment, Tokyo Institute of Technology, Japan 226-8502

³Professor, Dept. of Urban Environment and Systems, Chiba University, Japan 263-8522

⁴Satellite Business Division, PASCO Corporation, Japan 164-0001

Liu W., Matsuoka M., Yamazaki F., Nonaka T., Sasagawa T. Detection of Building Side-wall Damage Caused by The 2011 Tohoku, Japan Earthquake Tsunamis Using High-resolution SAR Imagery. *Proceedings of the 10th National Conference in Earthquake Engineering*, Earthquake Engineering Research Institute, Anchorage, AK, 2014.



Tenth U.S. National Conference on Earthquake Engineering
Frontiers of Earthquake Engineering
July 21-25, 2014
Anchorage, Alaska

Detection of Building Side-wall Damage Caused by The 2011 Tohoku, Japan Earthquake Tsunamis Using High-resolution SAR Imagery

W. Liu¹, M. Matsuoka², F. Yamazaki³, T. Nonaka⁴ and T. Sasagawa⁴

ABSTRACT

Building damage such as to side-walls or mid-story collapse is often overlooked in vertical optical images. Hence, in order to observe such building damage modes, high-resolution SAR images are introduced considering the side-looking nature of SAR. In the 2011 Tohoku, Japan, earthquake, a large number of buildings were collapsed or severely damaged due to repeated tsunamis. One of the important tsunami effects on buildings is that the damage is concentrated to their side-walls and lower stories. Thus, this paper proposes the method to detect this kind of damage from the change in layover areas in SAR intensity images. The pre- and post-event TerraSAR-X images covering the Sendai-Shiogama Port were employed to detect building damage due to the tsunamis caused by the earthquake. Firstly, shape data of the layover areas for individual buildings were made according to the 2D Zenrin GIS data because the lengths of layover are proportional to the building height. The characteristics of the difference of backscattering coefficients between the pre- and post-event images were investigated using several sample buildings. Then the average value and the gradient in the cumulative curve of the difference were used to classify the possibility of side-wall damage and the damage level of buildings. These examples demonstrated the usefulness of high-resolution SAR images to detect severe damage to building side-walls from the changes of the backscattering coefficient in layover areas. Finally, the method was applied to the whole target area, and the accuracy was verified by comparing with a building damage map made by field surveys.

Introduction

Remote sensing has been recognized as an efficient tool to monitor a wide range of the earth's surface in the normal time and in natural disasters. Damage detection of buildings soon after the occurrence of natural disasters is one of the important topics of satellite remote sensing. A number of studies have been conducted to identify damage situation of individual buildings from high-resolution multi-spectral sensors (e.g. QuickBird, Ikonos, WorldView-2) after damaging earthquakes in the world [1-3]. In these studies, the damage grades of buildings were judged from optical images captured from the vertical direction. Hence the building damages such as mid-story collapse or damage to side-walls were often overlooked because only the upper

¹Postdoctoral Fellow, Dept. of Built Environment, Tokyo Institute of Technology, Japan 226-8502

²Associate Professor, Dept. of Built Environment, Tokyo Institute of Technology, Japan 226-8502

³Professor, Dept. of Urban Environment and Systems, Chiba University, Japan 245-8522

⁴Satellite Business Division, PASCO Corporation, Japan 164-0001

surfaces of buildings could be seen and thus such types of damage modes were mostly invisible. The present authors [4] have proposed the use of building shadow lengths to detect mid-story collapse from optical satellite images. But this method cannot be applied in detecting damage to building side faces.

Although optical images can easily capture detailed ground surface information, the approach is limited by weather conditions. In contrast, synthetic aperture radar (SAR) sensing is independent of weather and daylight conditions, and thus more suitable for mapping damaged areas promptly. Due to remarkable improvements in radar sensors, high-resolution TerraSAR-X and COSMO-SkyMed SAR images are possible with ground resolution of 1 to 5 m, providing detailed surface information. The damage detection of urban areas using these high-resolution SAR images has become quite popular recently. Comparing the change in pre-event and post-event SAR intensity images, damage detection of buildings has been conducted several researchers [5-8]. Due to the side-looking nature of SAR, the layover of buildings and the multi-bounce of radar among the ground and buildings occur. These phenomena are significant in dense urban areas and then make damage identification of individual buildings difficult. However, if a building stands alone or faces to a wide street, the length of layover indicates the height of the building [9] and the status of its side-wall faces to the radar illumination direction. Utilizing the change in the backscattering intensity within the layover area of an individual building, this study attempts to detect the damage situation of building side-walls due to the 2011 Tohoku, Japan earthquake and tsunami.

The 2011 Tohoku, Japan Earthquake and TerraSAR-X Data Used

The Mw 9.0 Tohoku earthquake occurred on March 11, 2011, off the Pacific coast of northeastern (Tohoku) Japan, caused gigantic tsunamis, resulting in widespread devastation. The earthquake resulted from a thrust fault on the subduction zone plate boundary between the Pacific and North American plates. According to the GPS Earth Observation Network System (GEONET) at the Geospatial Information Authority (GSI) in Japan, crustal movements with maximums of 5.3 m to the horizontal (southeast) and 1.2 m to the vertical (downward) directions were observed over a wide area [10]. The earthquake triggered extremely high tsunamis of up to 40.5 m run-up in Miyako, Iwate Prefecture, and caused huge loss of human lives and destruction of infrastructure. According to the GSI, areas totaling approximately 561 km² were flooded by tsunamis following the earthquake [10]. Due to the huge tsunami, about 107 thousands buildings were washed away or collapsed. In this regard, the present authors [8] conducted the extraction of flooded areas due to the tsunami and identified washed-away buildings using the pre- and post-event TSX intensity images. Typical building damages due to the 2011 Tohoku earthquake tsunami in our field survey were shown in Fig. 1(a). The characteristic building damage by tsunami is that damage was occurred to building side-walls or lower parts, which is not the same with the damage caused by strong earthquake shaking. We try to detect this kind of damage to building side-walls using the side-looking nature of SAR. The strongest backscattering echoes from the side-walls and double-bounce with the ground may be reduced after this type of damage, as shown in Fig. 1(b-c).

The present authors [11] made a case study in the Sendai-Shiogama Port to investigate the characteristics of side-wall damaged buildings. The footprints of 13 damaged buildings and

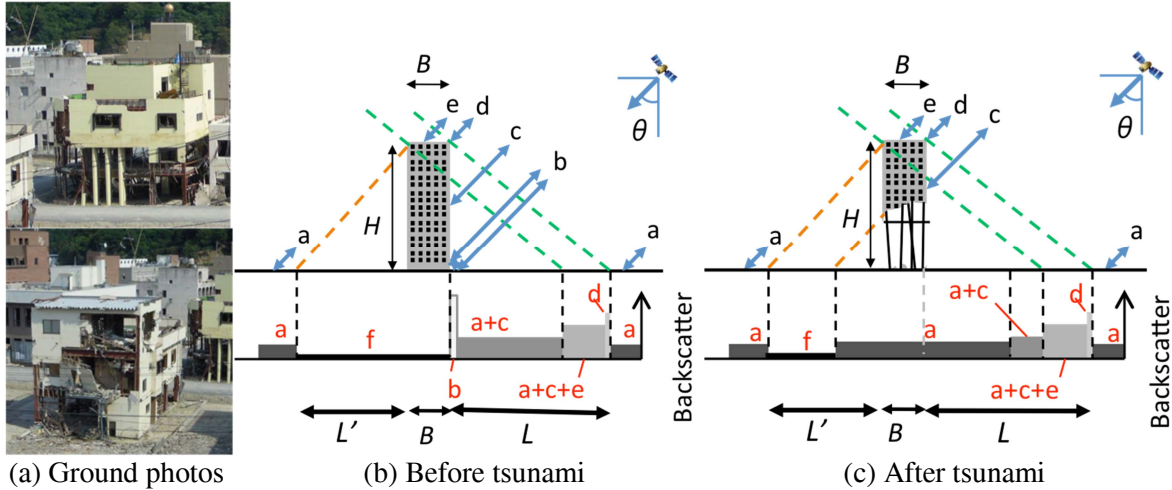


Figure 1. Typical tsunami damage to reinforced concrete and steel-frame buildings observed in our field survey after the 2011 Tohoku earthquake in Onagawa town (a); Schematic figure of SAR observation for an ideal tall flat-roof building, the amplitude of backscatter from an intact building (b), and the amplitude of backscatter from a damaged building due to tsunami (c).

13 non-damaged ones were built manually, and their layover areas were obtained by shifting the roof-top frames. It is observed that for the damaged buildings, the average backscattering coefficient within the layover area tends to be lower in the post-tsunami TSX images while the average value is almost unchanged for the non-damaged buildings. Thus, the changes of the backscattering coefficient in the layover areas are useful for detecting severe damage to building side-walls. However, the manual development of footprints costs time and labors, and hence it cannot be applied to a wide area. Thus, an automatic approach is necessary for the application of side-wall damage detection.

In this study, we focus on the coastal zone of Tohoku region, Japan, as shown in Fig. 2, which was one of the most severely affected areas during the 2011 Tohoku earthquake. Two TSX images taken before and three taken after the earthquake were used. We used them previously for detecting crustal movements [12], identifying flooded areas [8] and investigating the side-wall damages [11]. The pre-event image was taken on October 21, 2010 (local time), while the post-event one was April 4, 2011. The incidence angle was 37.3° at the center of the images. All the images were captured with HH polarization from a descending path. The images were acquired in the StripMap mode, and so the azimuth resolution was about 3.3 m while the ground range resolution was about 1.2 m. The images were orthorectified multi-look corrected products (EEC), where the image distortion caused by variable terrain height was compensated for by using a globally available DEM (SRTM). Therefore, they have been resampled and projected to a WGS84 reference ellipsoid with a square pixel size of 1.25 m.

Three preprocessing steps were applied to the images. First, the three TSX images were transformed to a Sigma Naught (σ^0) value, which represents the radar reflectivity per unit area in the ground range. Then an enhanced Lee filter was applied to the original SAR images to reduce the speckle noise, which makes the radiometric and textural aspects less efficient and improves the correlation coefficient between the two images. To minimize any loss of information

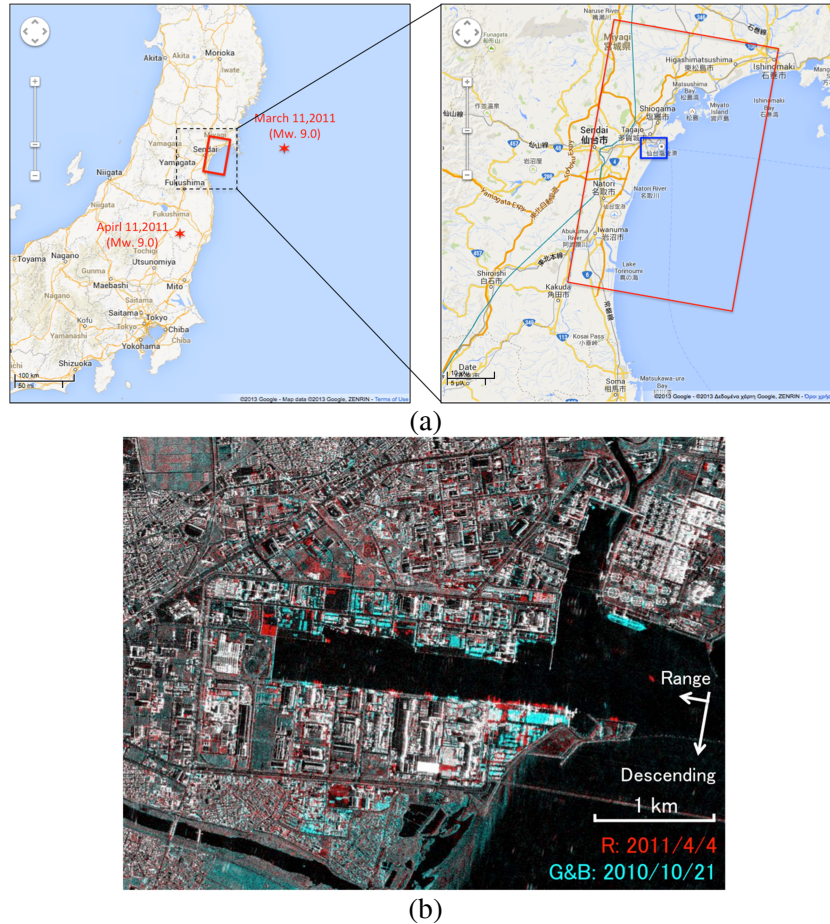
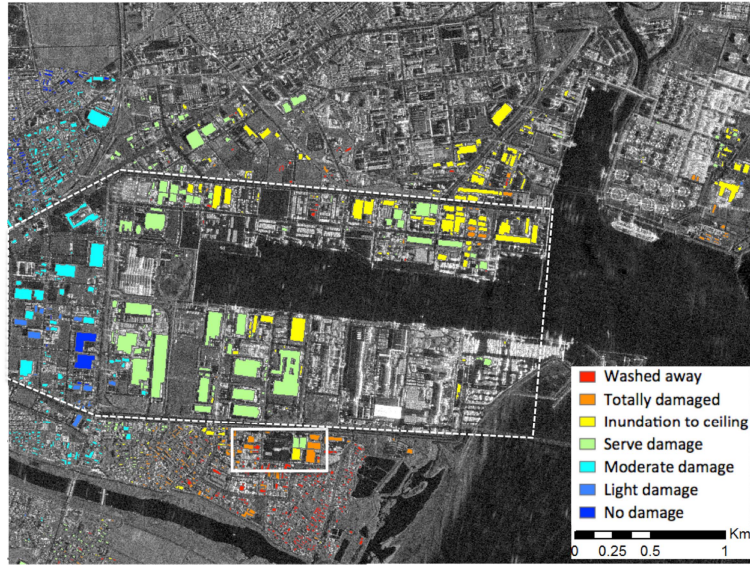


Figure 2. Study area along the Pacific coast of Tohoku, Japan with two target areas shown in blue frames (a); the color composites of the pre-processed TSX images in the target area of Sendai-Shiogama Port (b).

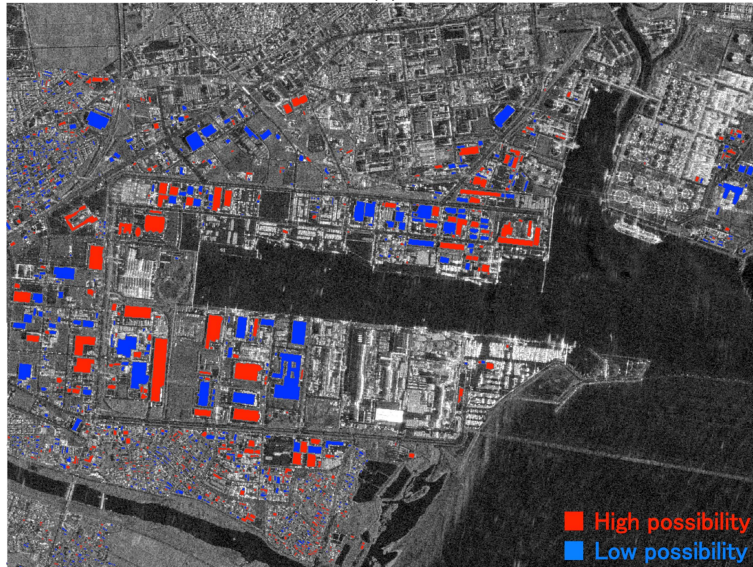
included in the intensity images, the window size of the Lee filter [13] was set as 3×3 pixels. The displacements caused by crustal movements when the post-event TSX images were taken were removed by coregistration at a sub-pixel level. The pre-processed images are shown in Fig. 2 (b) as a color composite, by loading the second image as red and the first image as green and blue. It is observed that the backscatter coefficients around the port decreased significantly and are shown in cyan color.

Detection of Building Side-wall Damage

To create the layover areas of buildings automated, the outlines of buildings data were cited from *Zenrin Product 2011* [14]. In addition, a building damage map made by field surveys was introduced from the reference [15], as shown in Fig. 3. In the damage map, buildings were classified into seven levels due to the damage conditions, “washed away”, “total damage”, “inundation up to ground floor’s ceiling”, “severe damage”, “moderate damage”, “light damage” and “no damage”. According to the criterion, the buildings with side-wall damage would be classified into “total damage”, “inundation up to ground floor’s ceiling”, and “severe damage”. In the previous case study area [11] within the solid line in Fig. 3, twelve of the 13 damaged



(a)



(b)

Figure 3. Building damage map of Sendai-Shiogama Port made by Ministry of Land, Infrastructure, Transport and Tourism of Japan, according to the field surveys [15] (a); the detected result of the possibility of side-walls damage (b).

buildings were classified as “total damage”, and one was as “inundation up to ground floor’s ceiling”. In this study, 245 buildings within the dotted line in Fig. 3 were selected as samples, including all the damage levels.

According to the side-looking nature of SAR sensor, the length of the layover area, L , can be calculated from the height of the building, H , as

$$L = H / \tan \theta \quad (1)$$

where θ is the incidence angle of SAR.

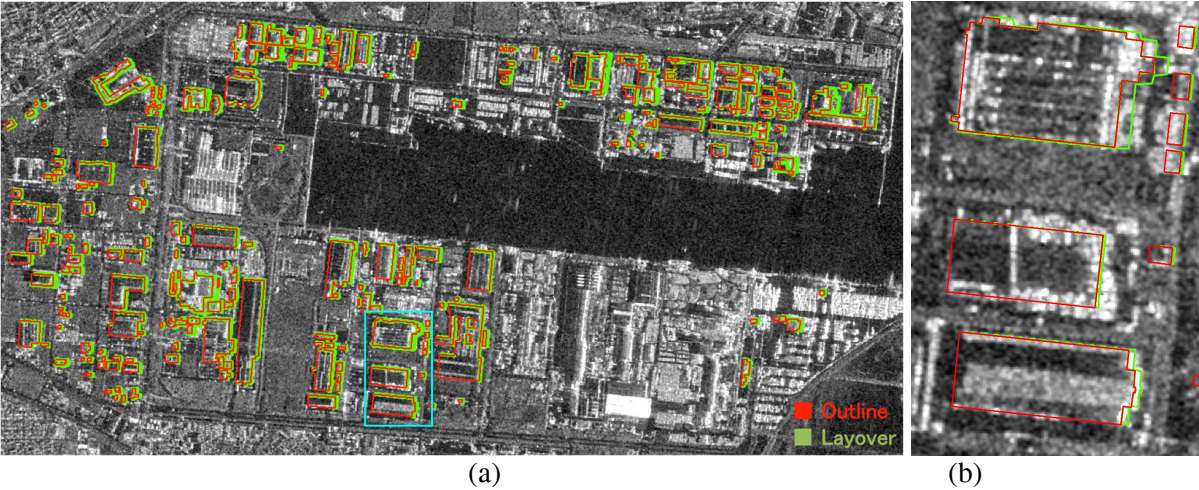


Figure 4. Building outlines cited from the damage map and the estimated layover areas (a); a close-up in the blue frame (b).

Although the heights of buildings are not included by the *Zenrin Product*, they can be estimated by multiplying 3 m to the number of stories which is included by the GIS data. For a two-storied building, the height was considered as 6 m and that the layover can be decomposed into 7.8 m to the east and 1.4 m to the south, according to the 37.3° incidence angle and the 190.4° heading angle clockwise from the north. All the layover areas of buildings were calculated, as shown in Fig. 4(a). A close up of the outline and the estimated layover area is shown in Fig. 4(b). For the three big buildings, the outlines and layovers look matched with the high backscattering coefficient areas in the TSX images.

In the previous study, the average value of the difference of backscattering coefficients between the pre- and post-event images within the layover area was used to identify side-wall damage. However, more discussions were carried out in this study. The cumulative distribution of the difference of backscattering coefficients within the layover was obtained from the 254 sample buildings, and shown in Fig. 5 (a-g). There are 11 buildings classified as washed away, 12 as total damage, 58 as inundation to ceiling, 80 as severe damage, 57 as moderate damage, 8 as light damage and 8 as no damage. It is observed that the gradients of the cumulative distributions in the moderate, light and no damage classes are higher than those in the wash away, totally damaged, inundation to ceiling and severe damage classes. As also observed in the previous study, the difference in those large damaged classes are lower than the light damaged classes. A graph of the distance (D) between the value when the cumulative probability reached 10% and the value of zero in the difference distribution of backscatter coefficients is shown in Fig. 5(h). Although the variation of D in each the damage class is large (around 4 dB), a decreasing trend can be confirmed as the damage level reduced. Thus, this characteristic was adopted as a parameter to identify the side-wall damage.

The side-wall damage and the damage level were detected by the average value and the distance D in the cumulative distribution of the difference within the layover areas. However, due to the large variation, D in the difference damage levels overlapped one another. It is difficult to define the threshold values from the sample buildings. Then, the discriminant analysis was used for the classification according to the Mahalanobis distance. For the 254 sample

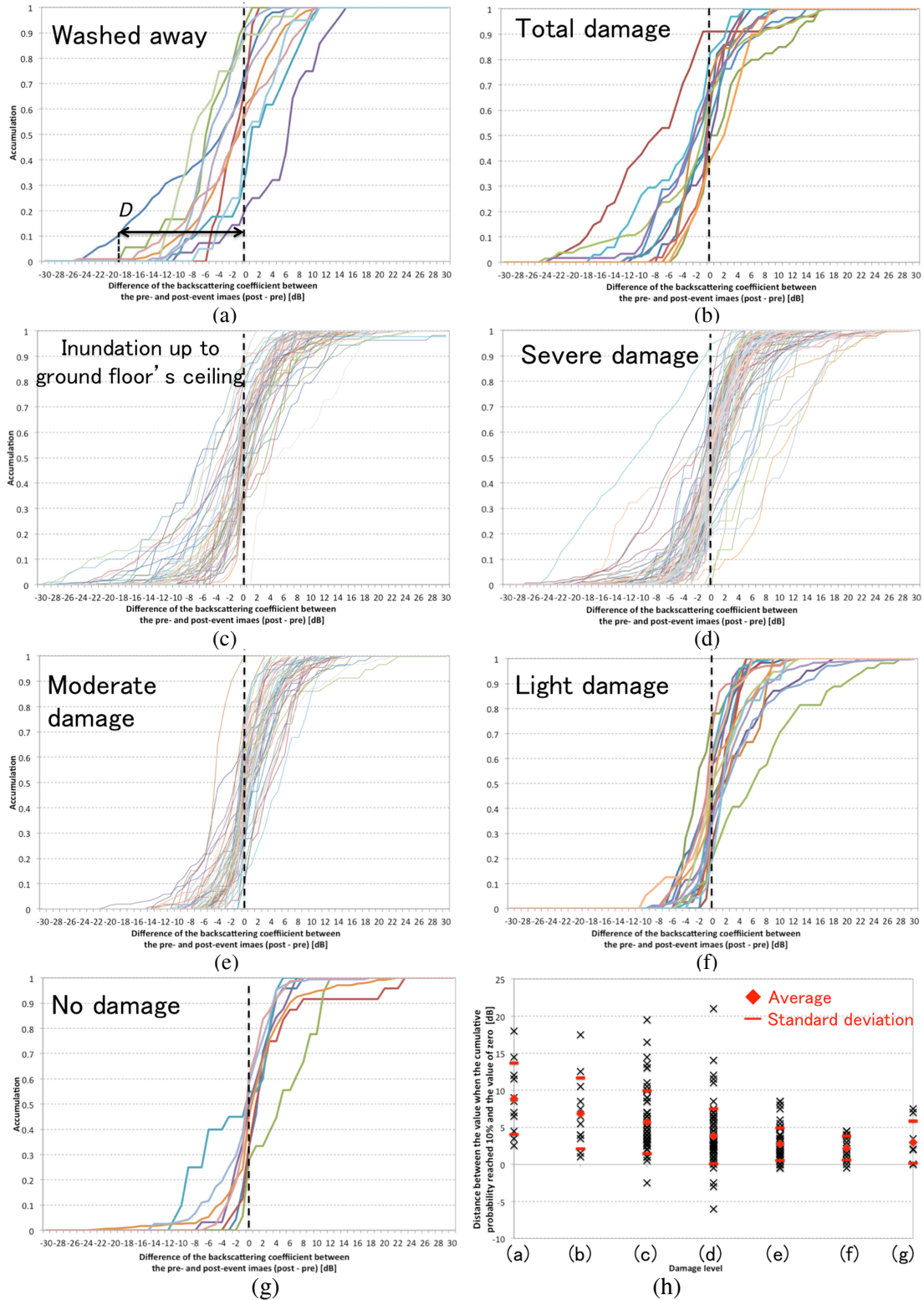


Figure 5. Cumulative distributions of the difference of backscattering coefficients between the pre- and post-event images within the layover areas in seven damage levels (a-g); the distance (D) between the value when the cumulative probability reached 10% and the value of zero in the difference distribution at seven damage levels (h).

buildings, the accuracy matrix was obtained by comparing with the reference and shown in Table 1(a). Since there is no significant difference in both the average and distance between two close damage levels, it is difficult to divide them completely. Thus, the discrimination into the neighboring damage levels was considered as correct. The accuracy of Table 1(a) was calculated using the grey cells. The overall accuracy for the sample buildings is 60%. However, the buildings could be only classified into damage or no damage using the average value of the difference, and they can be classified into different damage levels using the proposed method.

Table 1. Accuracy of the detection in the 245 sample buildings (a) and the building in the whole target areas (b), by comparing with the building damage map [15].

(a)

		Building damage map according to the field survey								User accuracy
		Washed away	Totally damaged	Inundation to ceiling	Severe damage	Moderate damage	Light damage	No damage	Total	
Detected results from the TSX images	Washed away	9	5	17	16	4	0	1	52	27%
	Totally damaged	0	0	1	5	1	0	1	8	13%
	Inundation to ceiling	0	2	7	5	2	0	0	16	88%
	Severe damage	2	3	17	19	24	12	2	79	76%
	Moderate damage	0	0	13	26	19	5	4	67	75%
	Light damage	0	2	3	9	7	1	0	22	36%
	No damage	0	0	1	0	0	0	0	1	0%
	Total	11	12	59	80	57	18	8	245	
	Producer accuracy	82%	58%	42%	63%	88%	33%	0%		60%

(b)

		Building damage map according to the field survey								User accuracy
		Washed away	Totally damaged	Inundation to ceiling	Severe damage	Moderate damage	Light damage	No damage	Total	
Detected results from the TSX images	Washed away	92	42	53	48	43	6	7	291	46%
	Totally damaged	12	13	12	12	21	1	4	75	49%
	Inundation to ceiling	13	5	15	19	25	4	5	86	45%
	Severe damage	75	53	63	72	90	22	20	395	57%
	Moderate damage	15	26	22	26	43	10	11	153	52%
	Light damage	9	2	8	11	24	2	5	61	51%
	No damage	0	0	0	0	0	1	0	1	100%
	Total	216	141	173	188	246	46	52	1062	
	Producer accuracy	48%	43%	52%	62%	64%	28%	0%		51%

The automatic discrimination according to the sample buildings was applied to all the buildings in the target areas shown in Fig. 3(a). The error matrix is shown in Table 1 (b). The overall accuracy is 51%, less than only applying on the sample buildings. Since the side-wall damaged buildings were classified into totally damaged, inundation to ceiling and severe damage in the building damage map, these classes in our detected result were considered as high possibility of side-wall damage, while the classes from the moderate damage to no damage were as low possibility. Then the possibility map of side-wall damage is shown in Fig. 3(b). The buildings with high possibility were located surrounding the port close to the sea. Twelve of the thirteen side-wall damaged buildings used in the case study were classified as high possibility, only one was misclassified as low possibility. When the accuracy was verified using only the classification of high and low possibility of side-wall damage, 71% buildings with high possibility can be detected and the producer accuracy of the detection is 83%.

The low accuracy comparing with the building damage map was caused by three reasons. First one is the accuracy of the outlines. As shown in Fig. 4(b), several outlines from the Zenrin product were not matched correctly with the buildings' location in the TSX images. Then the layover areas created according to the outlines did not include the backscatter of buildings' walls. The second reason is the complex surrounding conditions. Since several parking lots exist in the sensor direction of the target buildings, parking vehicles might be responsible for those temporary changes of backscatter. Thus, those buildings with no damage were classified as damaged incorrectly. The last reason can be considered as the observing direction of SAR. If the side-wall damage occurs to the opposite direction of the SAR sensor, no change could be observed in the backscatter. However, our detected results can provide positive information to improve the accuracy of damage classification using only satellite imagery or aerial photographs.

Conclusions

Building damage such as to side-walls or mid-story collapse is often overlooked in optical satellite images because the upper surfaces of buildings do not change too much in the vertical view. Hence, the use of high-resolution SAR intensity images is considered with the aid of side looking nature of SAR. In this paper, an automatic discrimination method to classify the building damage level and possibility of side-wall damage was proposed. The average value and the gradient in the cumulative distribution of the difference of backscattering coefficients between two temporal images were used as a parameter. Comparing with the building damage map made by field survey, the overall accuracy was more than 50%. However, our method could provide additional information for the rapid repose just after a disaster strikes.

Acknowledgments

The authors are grateful to Ministry of Land, Infrastructure and Transport (MLIT) of Japanese Government for their kind release of the Tohoku earthquake data. TerraSAR-X data are the property of German Aerospace Center (DLR) and the Inforterra GmbH, and provided by PASCO Corporation. This work was supported in part by a grant-in-aid for scientific research (Research No. 25003050; Principal Investigator: Masashi Matsuoka).

References

1. Yamazaki F., Yano Y., and Matsuoka M. Visual Damage Interpretation of Buildings in Bam City Using QuickBird Images Following the 2003 Bam, Iran, Earthquake. *Earthquake Spectra* 2005; 21(S1): S329-S336.
2. Ghosh S., Huyck C, K., Greene M., Gill S, P., Bevington J., Svekla W., DesRoches R., Onald R., Eguchi, T. Crowdsourcing for Rapid Damage Assessment: The Global Earth Observation Catastrophe Assessment Network (GEO-CAN). *Earthquake Spectra* 2011; 27(S1): S179-S198.
3. Miura H., Midorikawa S. and Kerle N. Detection of Building Damage Areas of the 2006 Central Java, Indonesia Earthquake through Digital Analysis of Optical Satellite Images. *Earthquake Spectra* 2012; 29(2): 453-473.
4. Iwasaki Y. and Yamazaki F. "Detection of building collapse from the shadow lengths in optical satellite images." *Proc. 32nd Asian Conference on Remote Sensing* 2011; 550-555.
5. Brunner D., Lemoine G. and Bruzzone L. "Earthquake damage assessment of buildings using VHR optical and SAR imagery." *IEEE Transactions on Geoscience and Remote Sensing* 2010; 48(5): 2403-2420.
6. Miura H. and Midorikawa S. "Preliminary Analysis for Building Damage Detection from High-Resolution SAR Images of the 2010 Haiti Earthquake." *Joint Conference Proceedings of 9th International Conference on Urban Earthquake Engineering and 4th Asia Conference on Earthquake Engineering* 2012; Paper No.01-212.
7. Uprety P. and Yamazaki F. Detection of Building Damage in the 2010 Haiti Earthquake using High-Resolution SAR Intensity Images. *Journal of Japan Association for Earthquake Engineering* 2012; 12(6): Special Issue, 21-35.
8. Liu W., Yamazaki F., Gokon H. and Koshimura S. Extraction of Tsunami-Flooded Areas and Damaged Buildings in the 2011 Tohoku-Oki Earthquake from TerraSAR-X Intensity Images. *Earthquake Spectra* 2013; 29(S1): S183-S200.
9. Liu W. and Yamazaki F. "Building height detection from high-resolution TerraSAR-X imagery and GIS data" *Proceedings of 2013 Joint Urban Remote Sensing Event* 2013; 33-36.
10. Geospatial information Authority of Japan. http://www.gsi.go.jp/BOUSAI/h23_tohoku.html
11. Yamazaki F., Iwasaki Y., Liu W., Nonaka T., and Sasagawa T. "Detection of damage to building side-walls in the 2011 Tohoku, Japan earthquake using high-resolution TerraSAR-X images." *SPIE Remote Sensing* 2013; CD-ROM, 9p.
12. Liu W. and Yamazaki F. Detection of crustal movement from TerraSAR-X intensity image. *IEEE Geoscience and Remote sensing Letters* 2013; 10(1): 199-203.
13. Lopes A., Touzi R. and Nezry E. Adaptive speckle filters and scene heterogeneity. *IEEE Transactions on Geoscience and Remote Sensing* 1990; 28(6): 992-1000.
14. Zenrin 2011. www.zenrin.co.jp
15. Ministry of Land, Infrastructure, Transport and Tourism of Japan. <http://fukkou.csis.u-tokyo.ac.jp/>